Two-Qubit Conditional Phase Gate in Laser-Excited Semiconductor Quantum Dots Using the Quantum Zeno Effect

K. J. Xu, Y. P. Huang, M. G. Moore, and C. Piermarocchi
Department of Physics & Astronomy, Michigan State University, East Lansing, Michigan 48824, USA
(Received 23 October 2008; published 14 July 2009)

We propose a scheme for a two-qubit conditional quantum Zeno phase gate for semiconductor quantum dots. The proposed system consists of two charged dots and one ancillary neutral dot driven by a laser pulse tuned to the exciton resonance. The primary decoherence mechanism is phonon-assisted exciton relaxation, which can be viewed as continuous monitoring by the environment. Because of the Zeno effect, a strong possibility of emission is sufficient to strongly modify the coherent dynamics, with negligible probability of actual emission. We solve analytically the master equation and simulate the dynamics of the system using a realistic set of parameters. In contrast to standard schemes, larger phonon relaxation rates increase the fidelity of the operations.

DOI: 10.1103/PhysRevLett.103.037401 PACS numbers: 78.67.Hc, 78.47.−p

The Quantum Zeno effect (QZE) [1–4] occurs when a rapid sequence of measurements is performed on a slowly evolving quantum system, with the result that the system is *frozen* in its initial state. An analogous effect occurs when a system is strongly coupled to a reservoir, as the transfer of information from the system into the reservoir mimics a continuous measurement. If coupling to the reservoir can be made contingent on the joint quantum state of two qubits, the QZE can be used in conjunction with control pulses to efficiently drive the qubits into an entangled state. This general approach has been discussed within the framework of interaction free measurements [5–7], decoherence free subspaces [8,9], as well as counterfactual quantum computation [10]. Proposed physical implementations vary from purely photonic systems [11–13], to atom-cavity systems [7,14], and superconducting qubits [15], yet without reported experimental realization.

Following a generalized QZE phase-gate recently proposed in [7], we have devised a two-qubit conditional phase gate using electron spins in semiconductor quantum dots. This system has the advantage over atomic systems that decoherence rates are of the order of picoseconds, which, in Zeno-based schemes, leads to significant improvements in gate time and/or fidelity. Moreover, here we can take advantage of both light-matter and electron-phonon interaction. We consider a system composed of three quantum dots (QDs), two of which are singly charged with electrons (see Fig. 1). The spins of these two electrons are then the logical qubits on which the phase-gate acts. A laser field is then applied, tuned to the exciton resonance of the uncharged dot. The energy levels and laser polarization are chosen so that the electron generated in the neutral dot will be spin up. If formed, the exciton can relax to the neighboring dots by a spin-conserving dissipative phonon-assisted process [16]. The emission of a phonon and relocation of the exciton would clearly indicate that at least one qubit spin did not match the electron spin of the exciton. Thus the possibility of phonon emission is equivalent to a strong continuous partial measurement [7,17] of the collective spin state of the two qubits.

Despite the widely-held belief that decoherence must always be minimized in quantum information processing, it has been known for some time [14] that decoherence can

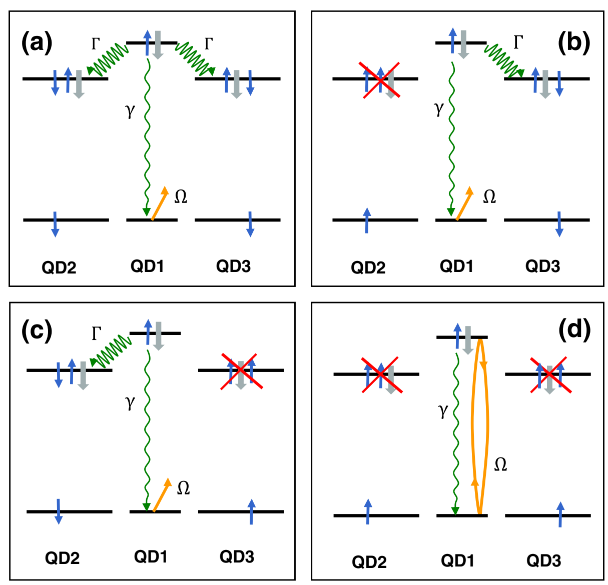

FIG. 1 (color online). Scheme of the dynamics of the system under different initial states. The narrow blue (bold gray) arrow represents the electron (hole) spins. The energy levels for QD1 are the empty dot (lower) and the first exciton level (upper), while the energy levels in QD2 and QD3 are charged dot ground states (lower) and trion states (upper). Figures (a)–(d) correspond to the four possible initial states of the two qubits. (a)–(c) If the electron in QD2 or QD3 is spin down, the exciton in QD1 can decay into one of the neighboring dots, in which case the QZE prevents the Rabi oscillation in QD1. (d) If both decay channels are closed, QD1 will undergo a 2π-Rabi oscillation. The photon-emission rate γ is too weak to induce a QZE.

in principle be harnessed to generate high-fidelity entanglement by use of the QZE. In our scheme, the QZE effect occurs when the strong dissipation rate of the exciton state suppresses the laser induced Rabi oscillations in the neutral dot, effectively freezing it in its ground state. As the dissipation mechanism is subject to Pauli blocking, the spin qubits in the charged dots can thus be seen as *quantum switches* that control the QZE. After a single Rabi cycle, a two level system will return to its original state times a π phase shift. In our system, only the up-up spin-qubit state undergoes Rabi oscillation, and acquires the -1 factor, thus realizing a conditional phase gate.

In order to predict the fidelity of state formation, we will use parameters appropriate for vertically grown (In, As)Ga/GaAs self-assembled quantum dots. Structures with vertically coupled neutral and charged quantum dots have been recently demonstrated [18]. Henceforth, the central neutral dot will be QD1, and the two lateral charged dots will be referred to as QD2 and QD3. Absorption of a photon creates an exciton state in QD1, and trion states in QD2 and QD3. We assume that the ground trion energies in the two lateral dots are similar, and are lower than the ground exciton energy in the central dot, so that phonon-mediated exciton relaxation is energetically allowed. In the absence of the QZE, the driving laser will induce Rabi Oscillations between the zero- and one-exciton states of QD1. Assuming that the driving laser field is σ_- polarized, the standard selection rules lead to the creation of an exciton with electron spin up ($+\frac{1}{2}$) and a heavy hole spin down ($-\frac{3}{2}$) in QD1. Because of the difference between the exciton and trion energy, QD2 and QD3 are far-detuned and thus not driven by the laser. The exciton and trion linewidths in InAs/GaAs quantum dots are of the order of 1 μeV [19]. Moreover, in our scheme we will use weak lasers so that both the Rabi energy and the linewidths are much smaller than the typical separation between the levels.

There are several exciton decay mechanisms that can spoil the Rabi oscillations. Many such processes depend on the intensity of the laser and have been experimentally characterized [20,21]. In the weak excitation limit, phonon-mediated processes are dominant. The role of the phonon is to carry away excess energy. For concreteness, we will assume that the phonon-assisted excitation transfer [16] is the dominant dissipation channel from QD1 to QD2 or QD3 since phonon-assisted relaxation of a *single* carrier between two dots via tunneling is exponentially suppressed for QD separations of several nm. Nonetheless, the scheme for the gate and our analytical results, can be easily adapted to the case in which QDs are close and the phonon emission involves only the electron. In this short-range case the energy levels of the central and lateral dots have to be engineered so that hole transfer is forbidden. For a weak resonant 2π laser pulse with Rabi energy $\Omega \ll \Gamma$, where Γ is the phonon emission rate, then the three spin states (up-down, down-up, and down-down) trigger the QZE and freeze the system. A schematic view of the different possible QZE scenarios for different initial states is shown in Fig. 1.

The quantum state of the system can be expressed in the triple-particle basis $|\lambda\sigma\sigma'\rangle = |\lambda\rangle_a \otimes |\sigma\sigma'\rangle_{23}$. Here, $|\lambda\rangle_a$ ($\lambda = 0, 1, 2, 3$) represents the state of the ancillary electron-hole pair created in QD1, where $\lambda = 0$ is the vacuum state with no exciton, while $\lambda = 1, 2, 3$ indicates the exciton residing in QD1, QD2, or QD3, respectively. $|\sigma\sigma'\rangle_{23}$ represents the combined state of the two logical qubits, with $\sigma, \sigma' \in \{\Uparrow, \Downarrow\}$ indicating the spin (up or down) states of the electrons in QD2 and QD3, respectively. The states $|2\Uparrow\sigma'\rangle$ and $|3\sigma\Uparrow\rangle$ are forbidden by the Pauli exclusion principle, and therefore excluded from our model.

Our goal is to realize a two-qubit phase gate for the electron spins in QD2 and QD3, with the electron-hole pair acting only as an ancillary system. Ideally, such a gate transforms an initial logical state $|\Psi_i\rangle_{23}$ of QD2 and QD3 to the final state $\hat{U}_\pi|\Psi_i\rangle_{23}$, with the π-phase-gate operator defined via $\hat{U}_\pi|\sigma\sigma'\rangle_{23} = (1 - 2\delta_{\sigma,\Uparrow}\delta_{\sigma',\Uparrow})|\sigma\sigma'\rangle_{23}$. The ancillary system, initially prepared in $|0\rangle_a$ state, becomes entangled with the logical qubits during the 2π pulse, becoming once again disentangled by the end of the pulse. Because of errors, the ancillary qubit might still be entangled with the logical qubits after the gate operation, so that the final density matrix representing QD2 and QD3 should be obtained by tracing over λ.

The system's Hamiltonian is given by

$$H = \epsilon_2 c_2^\dagger c_2 + \epsilon_3 c_3^\dagger c_3 + \frac{\Omega}{2}(c_1 + c_1^\dagger). \tag{1}$$

Here, the $c_i^\dagger(c_i)$ is the exciton creation (annihilation) operator, with $i = 1, 2, 3$ labeling the three QDs. Ω is the Rabi strength of the driving laser. In contrast to the state-selectivity of the phonon-mediated relaxation process, the decay of the exciton in QD1 via spontaneous photon emission is independent of QD2 and QD3 states, and will only cause the exciton to relax back to the initial $|0\rangle_a$ state. This is the primary source of error in the gate operation, and is mitigated by choosing $\Omega \gg \gamma$, where γ is the exciton spontaneous photon-emission rate.

To model the system's dynamics, we employ Linblad formalism [22] to arrive at the master equation

$$i\frac{\partial\rho}{\partial t} = -[\rho, H] + i\mathcal{L}[\rho], \tag{2}$$

where ρ is the density operator for the system. The super-operator $\mathcal{L}$ is given by

$$\mathcal{L}[\rho] = \frac{1}{2}\sum_{i=1}^{3}[L_i\rho L_i^\dagger - L_i^\dagger L_i\rho + \text{H.c.}], \tag{3}$$

where $L_1 = \sqrt{\gamma}c_1$ describes spontaneous photon decay in QD1, and $L_2 = \sqrt{\Gamma_2}c_2^\dagger c_1$, $L_3 = \sqrt{\Gamma_3}c_3^\dagger c_1$ describes phonon-assisted dissipation from QD1 to QD2 and QD3. Since the phonon-decay channels are independent, having a symmetric or asymmetric exciton decay rate will not significantly affect gate performance as long as $\Gamma_2, \Gamma_3 \gg \Omega$.

Thus, we choose $\Gamma_2 = \Gamma_3 = \Gamma$ for convenience. We note that other channels could as well be characterized by generalizing the Γ-terms to include any spin-selective relaxation channels, while γ-terms to include spin-independent ones.

During the gate operation, the system is initially in the state $\rho_i = |\Psi_i\rangle\langle\Psi_i| \otimes |0\rangle_a\langle 0|_a$, and then evolves under Eq. (2) for a duration of $t = 2\pi/\Omega$, resulting in a final density ρ_f. The fidelity is defined as

$$\mathcal{F} = \mathrm{tr}\{\rho_f \hat{U}_\pi |\Psi_i\rangle_{23}\langle\Psi_i|_{23}\hat{U}_\pi^\dagger \otimes \hat{P}_1\}, \tag{4}$$

where $\hat{P}_1 = |0\rangle_a\langle 0|_a + |1\rangle_a\langle 1|_a$. This gives the probability that two logical qubits are in the proper phase-gate output state with the electron-hole pair remaining in QD1. This later condition is required because relaxation of the exciton to either QD2 or QD3 results in a doubly charged dot and collapse of the two-qubit entangled state.

Before presenting numerical results, we first seek approximate analytical solutions to the dissipative dynamics of Eq. (2). Defining density matrices $\rho_{mn} = \langle m|_{23}\hat{P}_1\rho\hat{P}_1|n\rangle_{23}$, with $m, n \in \{\Uparrow\Uparrow, \Uparrow\Downarrow, \Downarrow\Uparrow, \Downarrow\Downarrow\}$, the master Eq. (2) can be divided into a set of uncoupled equations, leading to

$$\frac{\partial\rho_{mn}}{\partial t} = i[\rho_{mn}, H_0] + \frac{\gamma}{2}(c_1\rho_{mn}c_1^\dagger - c_1^\dagger c_1\rho_{mn} + \mathrm{H.c.}) - \alpha_m\Gamma c_1^\dagger c_1\rho_{mn} - \alpha_n\Gamma\rho_{mn}c_1^\dagger c_1, \tag{5}$$

where α_m is a logical-qubit dependent parameter, defined as $\alpha_m = 0, \frac{1}{2}, \frac{1}{2}, 1$, for $m = \Uparrow\Uparrow, \Uparrow\Downarrow, \Downarrow\Uparrow, \Downarrow\Downarrow$, respectively.

Successful operation requires $\Gamma \gg \Omega$ to impose the QZE, while $\gamma \ll \Omega$ is required to suppress spontaneous photon-emission, the primary failure mechanism. Hence, the operational range of the present Zeno phase gate is $\gamma \ll \Omega \ll \Gamma$. This separation of time-scales enables us to solve Eq. (5) perturbatively. With the definition $\rho_{mn}^{\lambda\lambda'} = \langle\lambda m|\rho|\lambda' n\rangle$, the matrix elements of the final density are given to second order in $\frac{\gamma}{\Omega}$ and $\frac{\Omega}{\Gamma}$ by $\rho_{mn}^{\lambda\lambda'} = \mu_{mn}^{\lambda\lambda'}\langle m|\Psi_i\rangle \times \langle\Psi_i|n\rangle$. The output coefficients $\mu_{mn}^{\lambda\lambda'}$ are given by Table I, with $f(x) = 1 - \frac{\pi}{2}x + \frac{3\pi^2}{50}x^2$, $g(x) = \frac{\pi}{100}x + \frac{3\pi^2}{500}x^2$. Note that the population and coherence dynamics in the subspace $\lambda = 2, 3$ are completely decoupled from the $\lambda = 0, 1$ subspace. In fact, we only need equations for the diagonal matrix elements with respect to the $\lambda = 0, 1$ subspace, as only they contribute to the fidelity (4). We see from Table I that to leading order, the gate output coefficients are consistent with only the state $|\Uparrow\Uparrow\rangle_{23}$ having acquired a π-phase shift, as desired for the π-phase gate.

TABLE I. Output coefficients.

m	n	μ_{mn}^{00}	μ_{mn}^{11}
$\Uparrow\Uparrow$	$\Uparrow\Uparrow$	$(1 + \frac{3\pi}{4}\frac{\gamma}{\Omega})^{-1}$	$1 - (1 + \frac{3\pi}{4}\frac{\gamma}{\Omega})^{-1}$
$\Uparrow\Uparrow$	$\neq\Uparrow\Uparrow$	$-f(\frac{\Omega}{\alpha_n\Gamma})\exp(-\frac{\pi}{2}\frac{\gamma}{\Omega})$	$g(\frac{\Omega}{\alpha_n\Gamma})(\frac{\gamma}{\Omega} + \pi\frac{\gamma^2}{\Omega^2})$
$\neq\Uparrow\Uparrow$	$\Uparrow\Uparrow$	$-f(\frac{\Omega}{\alpha_m\Gamma})\exp(-\frac{\pi}{2}\frac{\gamma}{\Omega})$	$g(\frac{\Omega}{\alpha_m\Gamma})(\frac{\gamma}{\Omega} + \pi\frac{\gamma^2}{\Omega^2})$
$\neq\Uparrow\Uparrow$	$\neq\Uparrow\Uparrow$	$\exp(-\frac{\pi}{2}\frac{\alpha_m+\alpha_n}{\alpha_m\alpha_n}\frac{\Omega}{\Gamma})$	0

The fidelity defined in Eq. (4) is now explicitly given by $\mathcal{F} = \sum_{mn}(-1)^{\delta_{m,\Uparrow\Uparrow}+\delta_{n,\Uparrow\Uparrow}}(\mu_{mn}^{00} + \mu_{mn}^{11})|\langle n|\Psi_i\rangle|^2|\langle m|\Psi_i\rangle|^2$, which depends on γ, Ω, Γ, as well as on the initial logical state $|\Psi_i\rangle$. In practice, while Γ and γ are known parameters for a given QD system, $|\Psi_i\rangle$ is in general arbitrary, making it impossible to simultaneously optimize Ω for all input states. For a given Ω, however, there is a lower bound $\mathcal{F}_{\mathrm{LB}}(\Omega) = \mathrm{Min}\{\mathcal{F}(\Omega), |\Psi_i\rangle \in \mathcal{H}\}$, where $\mathcal{H}$ is the full two-qubit Hilbert space. Maximizing the lower bound then gives $\mathcal{F}_{\mathrm{opt}} = \mathrm{Max}\{\mathcal{F}_{\mathrm{LB}}(\Omega), \forall\ \Omega\}$, for $\Omega_{\mathrm{opt}} = \sqrt{\gamma\Gamma/8}$ and

$$\mathcal{F}(\Omega_{\mathrm{opt}}) \geq \mathcal{F}_{\mathrm{opt}} = \exp\left[-\frac{10}{3}\sqrt{\frac{\gamma}{\Gamma}}\right], \tag{6}$$

so that the fidelity is improved only by increasing Γ/γ.

Considering recent theoretical calculations, the phonon-assisted transfer rate between two QDs can be as fast as several tens of picoseconds for favorable alignments [16]. The lifetime τ of the exciton in (In, As)Ga/GaAs QD is of the order of 1 ns [23], which only marginally meets our operational criteria. Nonetheless, τ can be significantly extended by embedding the QD system into an optical cavity. In fact, $\tau \sim 10$ ns has been demonstrated in a recent experiment [19]. For accessible parameters of $\Gamma = 20\ \mathrm{ns}^{-1}$, $\gamma = 0.08\ \mathrm{ns}^{-1}$, we find $\Omega_{\mathrm{opt}} = 0.45\ \mathrm{ns}^{-1}$ and $\mathcal{F}_{\mathrm{opt}} = 0.810$. For these parameters, we have also calculated the mean fidelity averaged over all the initial states as defined in Refs. [24,25], which gives $\mathcal{F}_{\mathrm{avg}} = 0.850$. As we will describe, a much higher fidelity can be obtained probabilistically by measuring the final state of the ancillary system to *herald* successful gate operation.

To verify the analytical results, we now solve exactly the dissipative dynamics Eq. (1) via numerical simulations. For comparison, we choose $\Gamma = 20\ \mathrm{ns}^{-1}$, $\gamma = 0.08\ \mathrm{ns}^{-1}$,

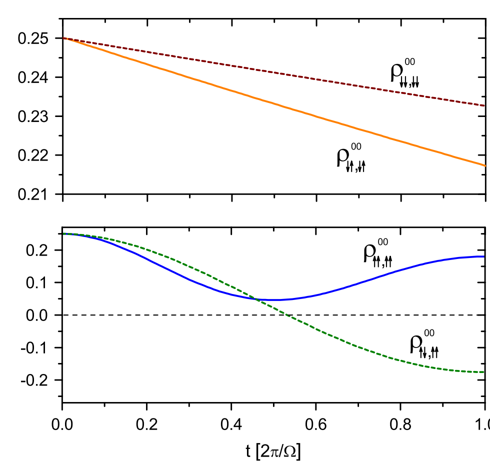

FIG. 2 (color online). Dynamical evolution of several density matrix elements for the initial state $|\Psi_i^0\rangle$ during the gate operation via numerical simulation.

$\Omega = 0.45\ \mathrm{ns}^{-1}$ and initial state $|\Psi_i^0\rangle = \frac{1}{2}(|\Uparrow\Uparrow\rangle + |\Uparrow\Downarrow\rangle + |\Downarrow\Uparrow\rangle + |\Downarrow\Downarrow\rangle)$. The dynamics of matrix elements $\rho^{00}_{\Uparrow\Uparrow,\Uparrow\Uparrow}$, $\rho^{00}_{\Downarrow\Downarrow,\Uparrow\Uparrow}$ and $\rho^{00}_{\Uparrow\Downarrow,\Downarrow\Uparrow}$, $\rho^{00}_{\Downarrow\Downarrow,\Downarrow\Downarrow}$ are shown in Fig. 2. From the figure we can see that both $\rho^{00}_{\Uparrow\Uparrow,\Uparrow\Uparrow}$ and $\rho^{00}_{\Downarrow\Downarrow,\Uparrow\Uparrow}$ undergo damped oscillation, due to $\gamma \ll \Omega$. At the end of the 2π-pulse, we find $\rho^{00}_{\Uparrow\Uparrow,\Uparrow\Uparrow} = 0.180$, and $\rho^{00}_{\Downarrow\Downarrow,\Uparrow\Uparrow} = -0.176$, compared with 0.176 and -0.175 respectively from the analytical results. The off-diagonal matrix element $\rho^{00}_{\Downarrow\Downarrow,\Uparrow\Uparrow}$ gains a minus sign after the 2π-pulse, which is the key ingredient of our phase gate. In contrast, both $\rho^{00}_{\Uparrow\Downarrow,\Downarrow\Uparrow}$ and $\rho^{00}_{\Downarrow\Downarrow,\Downarrow\Downarrow}$ are shown to be frozen in its initial state, due to QZE since $\Omega \ll \Gamma$. The final values of $\rho^{00}_{\Uparrow\Downarrow,\Downarrow\Uparrow}$ and $\rho^{00}_{\Downarrow\Downarrow,\Downarrow\Downarrow}$ are found to be 0.217 and 0.233, in agreement with the analytical results. The fidelity from the numerical simulation is with the initial state given above is 0.829, which is very close to the approximate analytical value of 0.831.

The gate fidelity can be further improved by measuring the final state of the ancillary electron-hole pair, which can "herald" successful gate operation. If it is detected in $|2\rangle_a$, $|3\rangle_a$ or $|1\rangle_a$ states, which correspond to a trion in QD2, QD3, or an exciton in QD1, failure is indicated. Only if the state $|0\rangle_a$ is obtained, is successful operation a possibility. In this case we obtain $\mathcal{F}_h = \mathcal{F}/(1 - P_f)$, where P_f is the failure probability. For the input state $|\Psi_i^0\rangle$, this heralded fidelity is $\mathcal{F}_h = 0.986$, a significant improvement from the unheralded value of 0.829. Similar improvements are found for other input states. The reason for the large improvement is that the dominant failure mechanism is photon emission via exciton decay in QD1. This is most likely to occur at the halfway point of gate operation, where the probability to have an exciton in QD1 reaches its maximum. This results in QD1 returning to $|0\rangle_a$ and begin a new Rabi oscillation cycle. In this scenario, only half of a Rabi cycle will have occurred, leaving QD1 in the exciton states. Thus gate failure will correlate highly with the ancillary system being found in state $|1\rangle_a$ at the end of gate operation.

In practice, the final state of the ancillary electron-hole pair might be measured by applying two driving lasers to the three QDs and detecting the resulting fluorescence photons. One of the lasers is tuned to be resonant with the trion and charged biexciton transition in QD2 and QD3, yet far-detuned from other transitions. Similarly, the other laser is resonant with the exciton and biexciton transition in QD1, and as well far-detuned from other transitions. A trion in QD2 and QD3, or an exciton in QD1, will then lead to resonance fluorescence, indicating the failure of the gate operation. On the other hand, the absence of fluorescence photons heralds the electron-hole being in the $|0\rangle_a$ state. We note that in the nonfluorescence case, the logical qubits are preserved, since they are driven far from resonance.

The results of this work demonstrate the possibility to realize a two-qubit controlled phase gate via the QZE in (In, As)Ga/GaAs self-assembled quantum dots. Using realistic values for all parameters, the obtained fidelity is around 0.85. If the final state of the exciton can successfully be measured, the heralded fidelity can be as high as 0.99. The fidelity can be improved further only if the phonon-assisted exciton transfer rate can and/or the lifetime of the exciton in the ancillary dot is increased. In principle, there could be different ways to scale our system to multiple qubits. For example, consider a chain of coupled cavities with one dot in each cavity. The ancillary dots will be off resonant with their cavity modes, so to reduce the γ, and the charged dots can be tuned in resonance to their cavity mode so to enhance the energy transfer rate Γ.

This work is supported in part by Nation Science Foundation Grants No. PHY0653373 and No. DMR0608501.

[1] B. Misra and E. C. G. Sudarshan, J. Math. Phys. (N.Y.) **18**, 756 (1977).
[2] C. B. Chiu, E. C. G. Sudarshan, and B. Misra, Phys. Rev. D **16**, 520 (1977).
[3] A. Peres, Am. J. Phys. **48**, 931 (1980).
[4] W. M. Itano, D. J. Heinzen, J. J. Bollinger, and D. J. Wineland, Phys. Rev. A **41**, 2295 (1990).
[5] P. Kwiat *et al.*, Phys. Rev. Lett. **74**, 4763 (1995).
[6] P. Horodecki, Phys. Rev. A **63**, 022108 (2001).
[7] Y. P. Huang and M. G. Moore, Phys. Rev. A **77**, 062332 (2008).
[8] P. Zanardi and M. Rasetti, Fortschritte Der Physik-Progess of Physics **48**, 559 (2000).
[9] P. Facchi and S. Pascazio, Phys. Rev. Lett. **89**, 080401 (2002).
[10] O. Hosten *et al.*, Nature (London) **439**, 949 (2006).
[11] J. D. Franson, B. C. Jacobs, and T. B. Pittman, Phys. Rev. A **70**, 062302 (2004).
[12] P. M. Leung and T. C. Ralph, Phys. Rev. A **74**, 062325 (2006).
[13] C. R. Myers and A. Gilchrist, Phys. Rev. A **75**, 052339 (2007).
[14] A. Beige, D. Braun, B. Tregenna, and P. L. Knight, Phys. Rev. Lett. **85**, 1762 (2000).
[15] X. B. Wang, J. Q. You, and F. Nori, Phys. Rev. A **77**, 062339 (2008).
[16] E. Rozbicki and P. Machnikowski, Phys. Rev. Lett. **100**, 027401 (2008).
[17] U. Hohenester, G. Pfanner, and M. Seliger, Phys. Rev. Lett. **99**, 047402 (2007).
[18] L. Robledo *et al.*, Science **320**, 772 (2008).
[19] K. Hennessy *et al.*, Nature (London) **445**, 896 (2007).
[20] T. H. Stievater *et al.*, Phys. Rev. Lett. **87**, 133603 (2001).
[21] Q. Q. Wang *et al.*, Phys. Rev. B **72**, 035306 (2005).
[22] P. Meystre, *Atom Optics* (Springer, New York, 2001).
[23] G. A. Narvaez, G. Bester, A. Franceschetti, and A. Zunger, Phys. Rev. B **74**, 205422 (2006).
[24] J. F. Poyatos, J. I. Cirac, and P. Zoller, Phys. Rev. Lett. **78**, 390 (1997).
[25] C. Piermarocchi, P. Chen, Y. S. Dale, and L. J. Sham, Phys. Rev. B **65**, 075307 (2002).